Research Article | Vol. 8, No. 3 | 1 Mar 2017 | BIOMEDICAL OPTICS EXPRESS 1405
Biomedical Optics EXPRESS

Hyperopic Q-optimized algorithms: a theoretical study on factors influencing optical quality

JOSE R. JIMÉNEZ,[1,*] AIXA ALARCÓN,[2] ROSARIO G. ANERA,[1] AND L. JIMÉNEZ DEL BARCO[1]

[1]*Departamento de Óptica, Facultad de Ciencias, Edificio Mecenas, Universidad de Granada, Spain*
[2]*Abbott Medical Optics, Groningen, The Netherlands*
[*]*jrjimene@ugr.es*

Abstract: In this work, we analyze the way in which pupil size, optical zone, and initial hyperopic level influence optical quality for hyperopic Q-optimized corneal refractive surgery. Different Q-optimized algorithms and the Munnerlyn formula were tested to analyze the optical quality of the final retinal image for initial hyperopic errors from 1D to 5D. Three optical zones (5.5, 6, and 6.5 mm) and two pupil diameters (5 and 7 mm) were considered. To evaluate optical quality, we computed the modulation transfer function (MTF) and the area under MTF (MTFa). Q-optimized values at around Q = –0.18 were found to provide the best optical quality for most of the conditions tested. This optimum final asphericity for hyperopic ablation was not depending on the degree of hyperopia corrected, the optical zone or the pupil size being this information important for clinical practice.

OCIS codes: (330.7335) Visual optics, refractive surgery; (170.4470) Ophthalmology; (330.7326) Visual optics, modeling.

References and links

1. S. Arba-Mosquera, M. C. Arbelaez, and D. J. DeOrtueta, "Laser corneal refractive surgery in the twenty-first century: a review of the impact of refractive surgery on high-order aberrations (and vice versa)," J. Mod. Opt. **57**(12), 1041–1074 (2010).
2. J. R. Jiménez, R. G. Anera, L. Jiménez del Barco, and L. Carretero, "Retinal image quality in myopic subjects after refractive surgery," J. Mod. Opt. **47**(9), 1587–1598 (2000).
3. J. R. Jiménez, F. Rodríguez-Marín, R. G. Anera, and L. Jiménez Del Barco, "Deviations of Lambert-Beer's law affect corneal refractive parameters after refractive surgery," Opt. Express **14**(12), 5411–5417 (2006).
4. D. Gatinel, J. Malet, T. Hoang-Xuan, and D. T. Azar, "Analysis of customized corneal ablations: theoretical limitations of increasing negative asphericity," Invest. Ophthalmol. Vis. Sci. **43**(4), 941–948 (2002).
5. C. Dorronsoro, D. Cano, J. Merayo-Lloves, and S. Marcos, "Experiments on PMMA models to predict the impact of corneal refractive surgery on corneal shape," Opt. Express **14**(13), 6142–6156 (2006).
6. S. Marcos, "Aberrations and visual performance following standard laser vision correction," J. Refract. Surg. **17**(5), S596–S601 (2001).
7. E. Moreno-Barriuso, J. M. Lloves, S. Marcos, R. Navarro, L. Llorente, and S. Barbero, "Ocular aberrations before and after myopic corneal refractive surgery: LASIK-induced changes measured with laser ray tracing," Invest. Ophthalmol. Vis. Sci. **42**(6), 1396–1403 (2001).
8. Y. C. Lee, F. R. Hu, and I. J. Wang, "Quality of vision after laser in situ keratomileusis: influence of dioptric correction and pupil size on visual function," J. Cataract Refract. Surg. **29**(4), 769–777 (2003).
9. M. Pop and Y. Payette, "Risk factors for night vision complaints after LASIK for myopia," Ophthalmology **111**(1), 3–10 (2004).
10. A. Alarcón, M. Rubiño, F. Pérez-Ocón, and J. R. Jiménez, "Theoretical analysis of the effect of pupil size, initial myopic level, and optical zone on quality of vision after corneal refractive surgery," J. Refract. Surg. **28**(12), 901–905 (2012).
11. C. C. Chen, A. Izadshenas, M. A. Rana, and D. T. Azar, "Corneal asphericity after hyperopic laser in situ keratomileusis," J. Cataract Refract. Surg. **28**(9), 1539–1545 (2002).
12. D. S. Durrie, R. T. Smith, G. O. Waring 4th, J. E. Stahl, and F. J. Schwendeman, "Comparing Conventional and Wavefront-Optimized LASIK for the Treatment of Hyperopia," J. Refract. Surg. **26**(5), 356–363 (2010).
13. L. Llorente, S. Barbero, J. Merayo, and S. Marcos, "Total and corneal optical aberrations induced by laser in situ keratomileusis for hyperopia," J. Refract. Surg. **20**(3), 203–216 (2004).

#283495 https://doi.org/10.1364/BOE.8.001405
Journal © 2017 Received 22 Dec 2016; accepted 2 Feb 2017; published 6 Feb 2017

Biomedical Optics EXPRESS

14. A. Nanba, S. Amano, T. Oshika, T. Uno, A. Toshino, Y. Ohashi, T. Yamaguchi, and T. Mihashi, "Corneal higher order wavefront aberrations after hyperopic laser in situ keratomileusis," J. Refract. Surg. **21**(1), 46–51 (2005).
15. D. de Ortueta, S. Arba Mosquera, and H. Baatz, "Aberration-Neutral Ablation Pattern in Hyperopic LASIK with the ESIRIS Laser Platform," J. Refract. Surg. **25**(2), 175–184 (2009).
16. A. J. Kanellopoulos, J. Conway, and L. H. Pe, "LASIK for hyperopia with the WaveLight excimer laser," J. Refract. Surg. **22**(1), 43–47 (2006).
17. J. Lian, W. Ye, D. Zhou, and K. Wang, "Laser in situ keratomileusis for correction of hyperopia and hyperopic astigmatism with the Technolas 117C," J. Refract. Surg. **18**(4), 435–438 (2002).
18. C. R. Munnerlyn, S. J. Koons, and J. Marshall, "Photorefractive keratectomy: a technique for laser refractive surgery," J. Cataract Refract. Surg. **14**(1), 46–52 (1988).
19. J. T. Lin, "Critical review on refractive surgical lasers," Opt. Eng. **34**(3), 668–675 (1995).
20. C. C. Chan and B. S. Boxer Wachler, "A comparison of CustomCornea myopia algorithms for wavefront-guided laser in situ keratomileusis," Arch. Ophthalmol. **126**(8), 1067–1070 (2008).
21. F. Manns, A. Ho, J. M. Parel, and W. Culbertson, "Ablation profiles for wavefront-guided correction of myopia and primary spherical aberration," J. Cataract Refract. Surg. **28**(5), 766–774 (2002).
22. J. A. Díaz, R. G. Anera, J. R. Jiménez, and L. Jiménez del Barco, "Optimum corneal asphericity of myopic eyes for refractive surgery," J. Mod. Opt. **50**(12), 1903–1915 (2003).
23. A. Amigó, S. Bonaque-González, and E. Guerras-Valera, "Control of induced spherical aberration in moderate hyperopic LASIK by customizing corneal asphericity," J. Refract. Surg. **31**(12), 802–806 (2015).
24. D. Myung, S. Schallhorn, and E. E. Manche, "Pupil size and LASIK: a review," J. Refract. Surg. **29**(11), 734–741 (2013).
25. A. Helgesen, J. Hjortdal, and N. Ehlers, "Pupil size and night vision disturbances after LASIK for myopia," Acta Ophthalmol. Scand. **82**(4), 454–460 (2004).
26. J. R. Jiménez, A. Alarcón, R. G. Anera, and L. Jiménez Del Barco, "Q-optimized algorithms: Theoretical analysis of factors influencing visual quality after myopic corneal refractive surgery," J. Refract. Surg. **32**(9), 612–617 (2016).
27. H. L. Liou and N. A. Brennan, "Anatomically accurate, finite model eye for optical modeling," J. Opt. Soc. Am. A **14**(8), 1684–1695 (1997).
28. J. R. Jiménez, R. G. Anera, and L. Jiménez del Barco, "Effects on visual function of approximations of the corneal-ablation profile during refractive surgery," Appl. Opt. **40**(13), 2200 (2001).
29. D. Gatinel, T. Hoang-Xuan, and D. T. Azar, "Volume Estimation of Excimer Laser Tissue Ablation for Correction of Spherical Myopia and Hyperopia," Invest. Ophthalmol. Vis. Sci. **43**(5), 1445–1449 (2002).
30. D. Gatinel, "LASIK for myopia, hyperopia and astigmatism," in *Refractive Surgery*, D.T. Azar, D. Gatinel and T. Hoang-Xuan, ed. (Mosby Elsevier, 2007).
31. J. R. Jiménez, R. G. Anera, J. A. Díaz, and F. Pérez-Ocón, "Corneal asphericity after refractive surgery when the Munnerlyn formula is applied," J. Opt. Soc. Am. A **21**(1), 98–103 (2004).
32. C. Dorronsoro, J. Siegel, L. Remon, and S. Marcos, "Suitability of Filofocon A and PMMA for experimental models in excimer laser ablation refractive surgery," Opt. Express **16**(25), 20955–20967 (2008).
33. J. R. Jiménez, F. Rodríguez-Marín, R. G. Anera, and L. Jiménez Del Barco, "Deviations of Lambert-Beer's law affect corneal refractive parameters after refractive surgery," Opt. Express **14**(12), 5411–5417 (2006).
34. C. Roberts, "Biomechanics of the cornea and wavefront-guided laser refractive surgery," J. Refract. Surg. **18**(5), S589–S592 (2002).
35. J. Schwiegerling and R. W. Snyder, "Corneal ablation patterns to correct for spherical aberration in photorefractive keratectomy," J. Cataract Refract. Surg. **26**(2), 214–221 (2000).
36. M. Dubbelman, V. A. D. P. Sicam, and G. L. Van der Heijde, "The shape of the anterior and posterior surface of the aging human cornea," Vision Res. **46**(6-7), 993–1001 (2006).
37. J. Polans, B. Jaeken, R. P. McNabb, P. Artal, and J. A. Izatt, "Wide-field optical model of the human eye with asymmetrically tilted and decentered lens that reproduces measured ocular aberrations," Optica **2**(2), 124–134 (2015).
38. R. G. Anera, J. R. Jiménez, L. Jiménez del Barco, and E. Hita, "Changes in corneal asphericity after laser refractive surgery, including reflection losses and nonnormal incidence upon the anterior cornea," Opt. Lett. **28**(6), 417–419 (2003).
39. P. Rosales and S. Marcos, "Customized computer models of eyes with intraocular lenses," Opt. Express **15**(5), 2204–2218 (2007).

1. Introduction

Of the many theoretical and experimental studies on visual quality after corneal refractive surgery, most refer to myopia [1–10] while fewer examine hyperopia [11–16]. As in myopia [1,6,7,10], experimental results on hyperopic correction show a decline in best-corrected visual quality after corneal surgery, with a post-surgical increase in corneal and total aberrations [13,14] as well as a deterioration in contrast sensitivity [12]. Some patients also

Biomedical Optics EXPRESS

usually mention night-vision disturbances (NVDs), such as halos and glare, after hyperopic corneal refractive [17].

New ablation algorithms have been proposed to improve visual quality after corneal surgery as well as to minimize NVDs. The Munnerlyn formula [18,19] has been replaced by algorithms such as wavefront-guided [20], wavefront-optimized [12] and Q-optimized [21–23] (with fixed post-operative corneal asphericity Q) that provide better results on visual quality.

The role of different variables in visual quality after surgery is under discussion. For example, different works [9,10,24–26] have analyzed the relation of the optical zone, pupil size, and the initial degree of myopia to visual quality and NVD after myopic surgery. In this paper, we undertake a theoretical study on the role of pupil size, optical zone, and initial hyperopic level in hyperopic Q-optimized algorithms. We test different post-operative Q values and compare the results with those found using the Munnerlyn formula. This is the first study available that provides a theoretical analysis on this topic and it can be useful in clinical practice in order to choose the final Q value for hyperopic surgery based on different variables, such as optical zone, pupil size, and initial degree of hyperopia.

2. Method

Here, we used the eye model proposed by Liou and Brennan [27] to simulate hyperopic eyes. This model tries to predict the spherical and chromatic aberrations, as closely as possible to empirical results. The model provides values of $Z_{4,0}(\mu m) = 0.095$ and $Z_{4,0}(\mu m) = 0.211$ for ocular and corneal spherical aberration, respectively, in the case of a pupil diameter of 6.0 mm. The axial length of the model was modified to provide the initial degree of hyperopia, from 1D to 5D, a range usually used in hyperopic surgery [11–16]. Eye models slightly modified to simulate ametropia have been used in the myopia simulations [2,28]. Zemax OpticStudio 16 (ZEMAX Development Corp. Bellevue, Washington, USA) was used for the computations.

The ablation depth for the hyperopic correction, s(y), provided by the Munnerlyn formula (which considers the anterior cornea as a sphere) is given by [18,19,29]:

$$s(y) = \sqrt{R_1^2 - y^2} - \sqrt{R_2^2 - y^2} + R_2 - R_1 \tag{1}$$

with R_1 and R_2 being the radius pre- and post-surgery, respectively, and y is the radial distance from the optical axis. Equation (1) fulfills the required conditions s(0) = 0 for hyperopia [29]. In the case that we consider the eye to be a conic curve (described by radius and corneal asphericity), after simple computations [2,28] and imposing the condition s(0) = 0, we would have the following equation for the ablation depth, s(y):

$$s(y) = \frac{1}{1+Q_1}\sqrt{\left(R_1^2 - y^2(1+Q_1)\right)} - \frac{1}{1+Q_2}\sqrt{\left(R_2^2 - y^2(1+Q_2)\right)} + \frac{R_2}{1+Q_2} - \frac{R_1}{1+Q_1} \tag{2}$$

with Q_1 and Q_2 being the pre-surgical and post-surgical corneal asphericity, respectively. Equations (1) and (2) are equal for $Q_1 = Q_2 = 0$, as expected. For both equations the number of diopters to correct, D, is related to the pre-surgical and post-surgical radius (R_1 and R_2, respectively) as follows [18,19]:

$$\frac{D}{0.375} = \frac{1}{R_2} - \frac{1}{R_1} \tag{3}$$

In Eqs. (1) and (2), we chose $R_1 = 7.77$ mm and $Q_1 = -0.18$ values provided by the Liou and Brennan's schematic eye model [27]. Post-surgical R_2 was determined from the initial degree of hyperopia to correct using Eq. (2).

Biomedical Optics EXPRESS

We tested four different Q_2 values chosen from those proposed by different models: Q_2 = 0.0 used in some aspheric algorithms [23] to offset the negative spherical aberration induced by hyperopic ablation; Q_2 = −0.18 provided by the model of Liou and Brennan [27] as an average asphericity; Q_2 = −0.45, given by Manns et al. [21] for targeting zero primary spherical aberrations, this criterion being used in algorithms such as CIPTA (Corneal Interactive Programmed Topographic Ablation; Ligi Custom Refractive Technologies, Taranto, Italy); and Q_2 = −0.60, a Q-value calculated by an algorithm that optimizes the RMS spot size [22]. The results for the four different Q-algorithms tested were compared with those found using the Munnerlyn formula, Eq. (1).

Ablation algorithms, Eqs. (1) and (2), were applied in the central zone of the anterior cornea to correct for the hyperopic error. The transition zone was selected as is usual in hyperopia [30]. The ablated surface and the original cornea were connected with a transition divided into two zones (concave and convex) to connect smoothly ablated and non-ablated zones. Third-degree polynomials were used to create this smooth transition.

To evaluate the image quality, we computed the modulated transfer function (MTF) and the area under the MTF from 0 to 60 cycles per degree (MTFa). All calculations were performed at a wavelength of 555nm.

Simulations were performed for a range of initial hyperopia values (from 1D to 5D), using three different sizes of the optical zone (5.5 mm, 6 mm, and 6.5mm). In all cases, we used a transition zone of 2.5 mm. Two different pupil sizes, one smaller than the optical zone (5 mm) and the other greater than the optical zone (7mm), were tested. We also made tests for 4 mm of pupil size but we verified that the trends in the results were similar to those found for the 5-mm pupil size. Our aim was to evaluate how these variables (initial degree of hyperopia, optical zone, and pupil size) can affect the final optical quality and the Q-algorithm selection.

3. Results

Figure 1 shows MTF curves for a hyperopic correction of 2D and for an optical zone of 5.5 mm with a) pupil of 5 mm and b) pupil of 7 mm; optical zone of 6.5 mm: c) pupil of 5 mm and d) pupil of 7 mm. MTF curves show that for low-medium frequencies (approx. 0-35 cpd) the Munnerlyn algorithm provides the best results while for high frequencies (>35 cpd) the algorithm Q = −0.18 offers better MTF. This occurs for a pupil size larger and smaller than the optical zone tested. Similar results were found for an optical zone of 6 mm.

Biomedical Optics EXPRESS

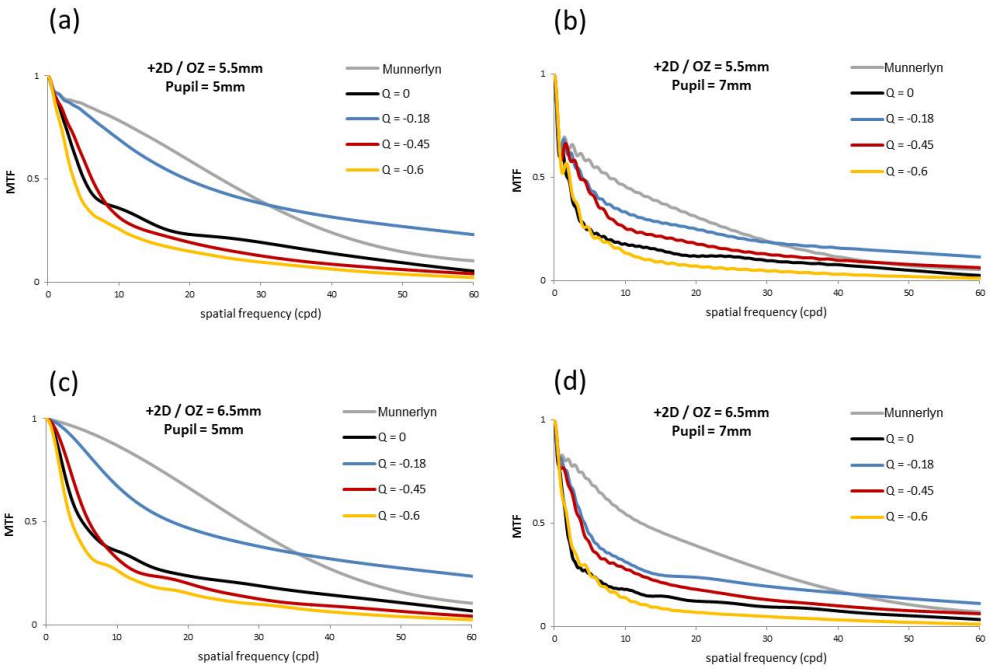

Fig. 1. . MTF as a function of spatial frequency in cycles per degree (cpd) for 2D hyperopic correction for different Q-optimized algorithms and the Munnerlyn formula. Optical zone 5.5 mm: (a) pupil 5 mm and (b) pupil 7 mm. Optical zone 6.5 mm: (c) pupil 5 mm and (d) pupil 7 mm.

Figure 2 shows the MTF for a hyperopic correction of 5D for an optical zone of 5.5 mm with a) a pupil size of 5 mm and b) a pupil size of 7 mm; and for an optical zone of 6.5 mm with a) a pupil size of 5 mm and b) a pupil size of 7 mm. For lower frequencies of around 20 cpd the Munnerlyn formula provides the best results, while Q = –0.18 provides the best results for higher frequencies. These trends found for 2D and 5D were similar for other hyperopic corrections.

Biomedical Optics EXPRESS

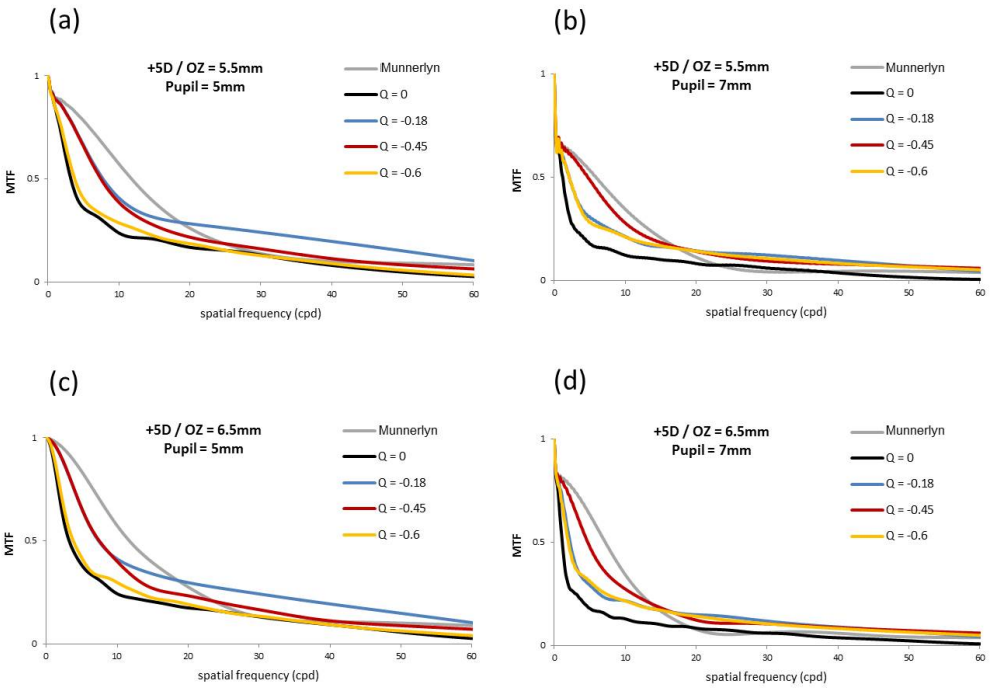

Fig. 2. . MTF as a function of spatial frequency in cycles per degree (cpd) for 5D hyperopic correction for different Q-optimized algorithms and the Munnerlyn formula. Optical zone 5.5 mm: (a) Pupil 5 mm and (b) Pupil 7 mm. Optical zone 6.5 mm: (c) pupil 5 mm and (d) pupil 7 mm.

More complete MTF information is provided by the MTFa (area under MTF). Figure 3 shows the MTFa curves for all the conditions tested: three optical zones and the whole range of corrected diopters. For a pupil size of 5 mm, smaller than the optical zone, in all the ablation zones tested, the Munnerlyn formula and Q = –0.18 provide the best results for the entire range of diopters (1D-5D). From 2.5D, the Q = –0.18 algorithm provided the best results; in the range 1D-2.5D the Munnerlyn formula gave the best results in two cases (optical zones of 6 mm and 6.5 mm) and Q = –0.18 for the case of an optical zone of 5.5 mm.

For a pupil of 7 mm (larger than the optical zone), the Munnerlyn formula offered the best results for a hyperopia degree up to 4.5D, while Q = –0.18 provided the second-best results. In the range 4.5D-5D, the Munnerlyn formula, Q = –0.18 and Q = –0.45, provided similar MTFa values.

Biomedical Optics EXPRESS

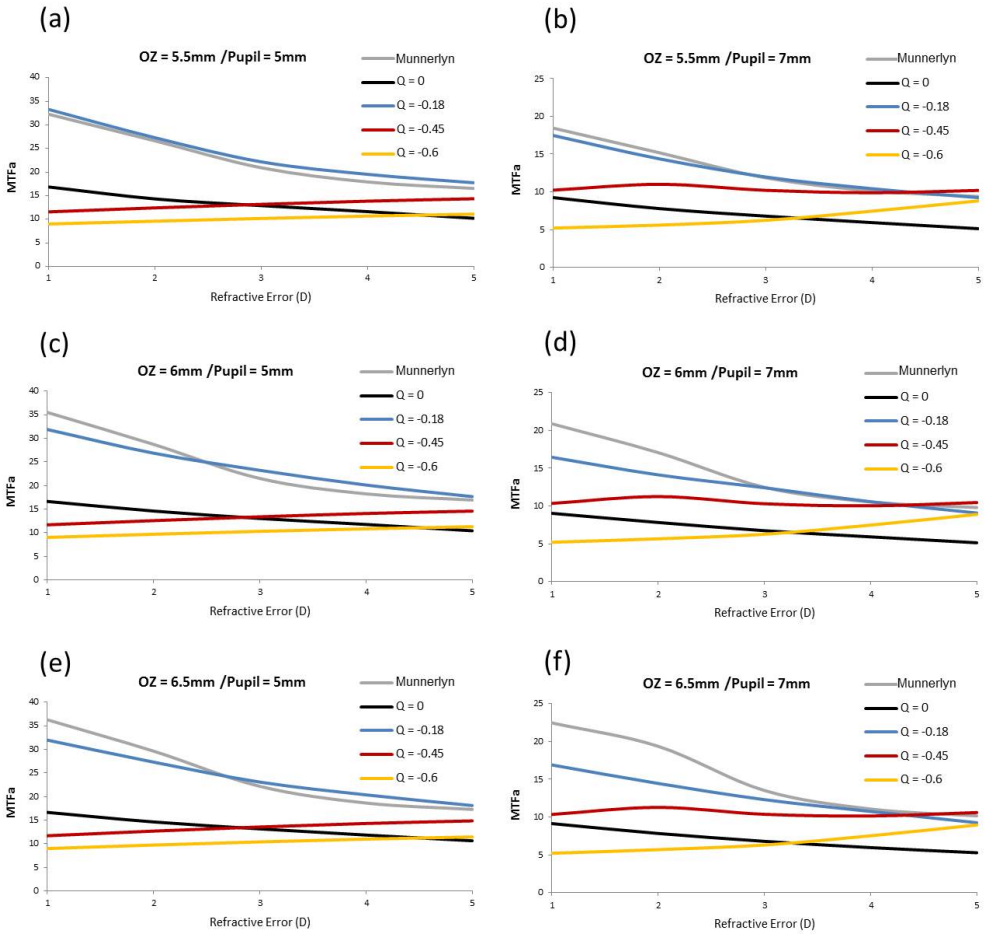

Fig. 3. Area under the MTF (MTFa) as a function of the level of hyperopic correction for different Q-optimized algorithms and the paraxial Munnerlyn formula. (a) MTFa for 5-mm pupil and 5.5 mm of optical zone; (b) MTFa for 7-mm pupil and 5.5 mm of optical zone; (c) MTFa for 5-mm pupil and 6 mm of optical zone; (d) MTFa for a 7-mm pupil and 6 mm of optical zone; (e) MTFa for a 5-mm pupil and 6.5 mm of optical zone; (f) MTFa for a 7-mm pupil and 6.5 mm of optical zone.

4. Discussion

This study evaluates the effect of pupil size, optical zone, and initial hyperopic level on optical quality for hyperopic Q-optimized corneal refractive surgery. For this, we tested different post-operative Q values and compared the results with those found using the Munnerlyn formula.

The first unexpected finding was that the Munnerlyn formula provided the best results for MTFa under a high percentage of conditions tested. It should be noted that the proposal of new algorithms in refractive surgery was justified by the worse visual quality provided by the non-optimized algorithms based on the Munnerlyn formula. An analysis of the post-surgical corneal asphericity for hyperopia when the Munnerlyn formula is used may explain these results.

Theoretic post-surgical asphericity, Q_2, using the Munnerlyn formula is given by [31]:

Biomedical Optics EXPRESS

$$Q_2 = \left(\frac{R_2}{R_1}\right)^3 Q_1 \tag{4}$$

Equation (4) was deduced considering only the ablation algorithm. Other potential variables that influence corneal ablation such as the physical aspects of ablation, biomechanical effects [1,32–34] and different transition zones [35] were not considered. Analyzing Eq. (4), we observe that the post-surgical asphericity depends strongly on pre-surgical asphericity, Q_1, and varies with the degree of hypermetropia corrected. In our case, the pre-surgery asphericity was $Q_1 = -0.18$, whereas on applying Eq. (4) for the range of hyperopia studied (1D-5D), we got a post-surgical asphericity ranging from $Q = -0.18$ to $Q = -0.15$. Therefore, we find that the Munnerlyn formula provides values similar to those of the case $Q = -0.18$, giving a maximum difference in asphericity with respect to the algorithm $Q = -0.18$ of $\Delta Q = 0.03$ for 5D of initial hyperopia.

Therefore, the good results found with the Munnerlyn algorithm appear to be due to the initial asphericity, $Q_1 = -0.18$, from the model of Liou and Brennan [27]. Thus, we repeated the calculations modifying the value of the initial asphericity. For this, we took two initial asphericity values $Q_1 = 0$ and $Q_1 = -0.40$ (one higher and one lower than $Q_1 = -0.18$). Figure 4 shows the results of MTFa for $Q_1 = 0$ (a and b) and $Q_1 = -0.40$ (c and d) for different Q_2 and an optical-zone diameter of 6 mm (similar results were found for an optical-zone diameter of 5.5 and 6.5 mm).

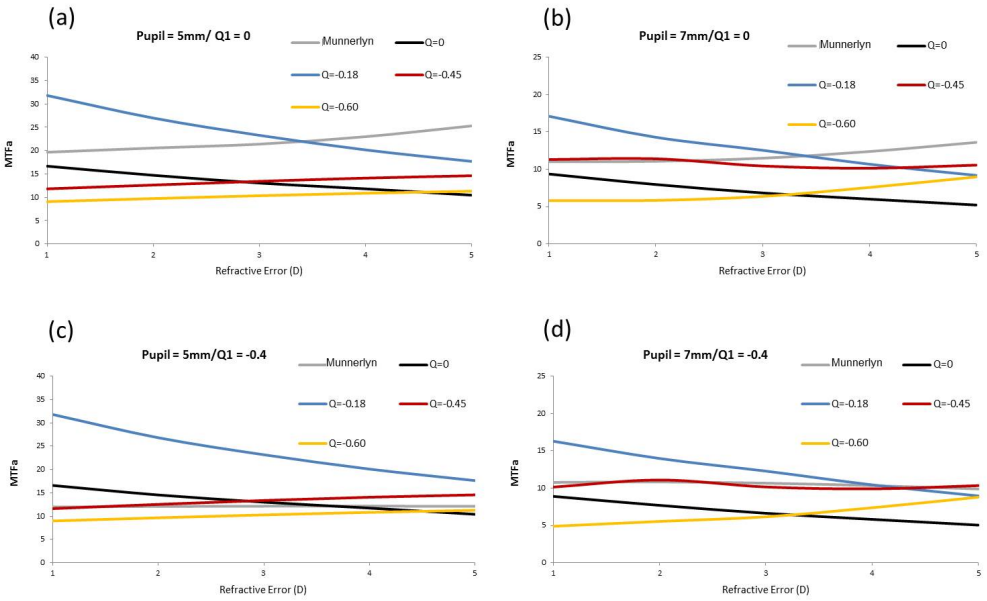

Fig. 4. Area under the MTF (MTFa) as a function of the level of hyperopic correction for different Q-optimized algorithms and the paraxial Munnerlyn formula for 6mm of optical zone: (a) MTFa for pre-surgery asphericity $Q_1 = 0.0$ and 5-mm pupil; (b) MTFa for pre-surgery asphericity $Q_1 = 0.0$ and 7-mm pupil; (c) MTFa for pre-surgery asphericity $Q_1 = -0.4$ and 5-mm pupil; (d) MTFa for pre-surgery asphericity $Q_1 = -0.4$- and 7mm pupil.

Figure 4 shows that, regardless of the pupil size, $Q_2 = -0.18$ continued to provide the best MTFa results in most conditions, especially for a more prolate initial cornea ($Q_1 = -0.40$). Only for $Q_1 = 0$ and refractive errors greater than 3.5D, did the Munnerlyn algorithm offer better results than $Q_2 = -0.18$. Therefore, the final asphericity value $Q_2 = -0.18$ provided the best results under most of the conditions tested. As expected, the Munnerlyn formula did not

Biomedical Optics EXPRESS

provide the excellent results achieved with an initial asphericity of $Q_1 = -0.18$, the image quality strongly decreasing when the initial asphericity was varied, especially towards more negative values.

Although the posterior surface of the cornea and the lens are not directly altered during refractive surgery, they are surfaces that influence eye aberrations. With the aim of making the results of this work independent from the fixed values selected in the model of Liou and Brennan [27], we proceeded with the same calculations but using theoretical variations in the asphericity parameters of the posterior cornea and the asphericity of the lens (both anterior and posterior). For the posterior surface of the cornea, the Liou and Brennan model assumes a value of $Q = -0.6$; experimental data [36] on corneal asphericity of the posterior cornea show a range of $Q = -0.4$ to $Q = -0.1$ for most of the experimental values in a wide range of ages. We repeated the calculations for posterior cornea assaying the values from $Q = -0.4$ to $Q = -0.1$ in steps of 0.1 while maintaining the other eye parameters of the Liou and Brennan model constant and, of course, the different degrees of initial hyperopia assayed.

With respect to the lens, we repeated the calculations testing the data of the lens asphericity of the recent model of Polans et al. [37]. In this model the asphericity of the anterior and posterior lens were $Q = -0.19$ and $Q = 0.82$, respectively. To introduce greater variability in the values of the lens, we also made calculations increasing/diminishing ($\pm \Delta Q = 0.2$) the asphericity values of the lens model of Polans et al. [37] in steps of 0.1. Also, we made the calculations with simultaneous combinations of variations assayed in the corneal and lens asphericity (anterior and posterior). We believe that these variations include a large quantity of values of aberrations of the cornea, lens, and total eye that may reflect a potentially broad range of individual variations in aberrations.

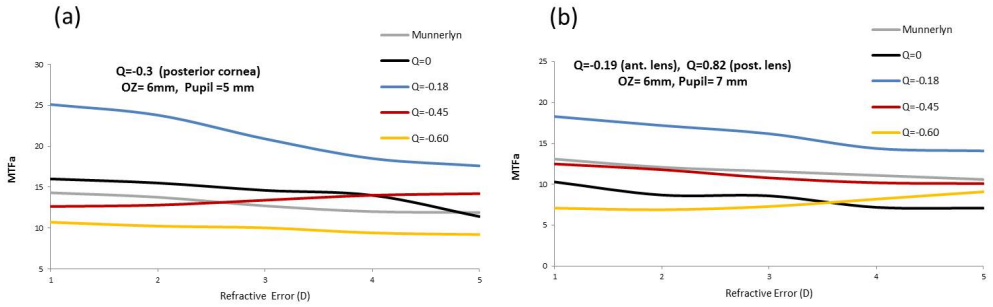

Fig. 5. Area under the MTF (MTFa) as a function of the level of hyperopic correction for different Q-optimized algorithms and the paraxial Munnerlyn formula for 6mm of optical zone: (a) MTFa for pre-surgery posterior-cornea asphericity $Q = -0.3$ and 5-mm pupil; (b) MTFa for pre-surgery anterior-lens asphericity $Q = -0.19$, posterior-lens asphericity $Q = 0.82$ and 7-mm pupil.

Figure 5 shows the results for two of the conditions assayed: (a) $Q = -0.3$ for posterior cornea and (b) $Q = -0.19$ for anterior lens and $Q = 0.82$ for posterior lens. The results show no changes in the post-surgical trends, the value remaining at around $Q = -0.18$ as the post-surgical value of corneal asphericity that provides the best results in most of the cases that we assayed (variations in asphericity of the posterior cornea and the lens, anterior and posterior).

For hyperopia, we found that, for post-surgery asphericity values of around $Q = -0.18$, visual quality optimized under a broad variety of conditions: different optical-ablation zones and for pupils larger or smaller than the ablation zone. These results differ with respect to a similar study made on myopia [26]. The controversy surrounding the role of the pupil, optical zone, and the degree of initial myopia in relation to post-surgical visual quality is well known. A theoretic study [26] was conducted to verify whether the Q-optimized algorithm provides better quality. This study reported that it is not possible to have a final Q that optimizes visual

Biomedical Optics EXPRESS

quality for all pupil size, optical zone, or initial degree of myopia, depending strongly on that optimization of these variables. In the case of hyperopia, our results showed that a value of around Q = –0.18 gave the best results under a great variety of experimental conditions. This result has far-reaching practical implications for a patient operated on for hyperopia.

The present work does not take into account the effects of other variables influencing real hyperopic ablation, such as the physical and biomechanical effects, ageing effects and temporal changes in cornea and lens after surgery. For example, it is known that biomechanical effects could cause a deviation between expected and real corneal asphericity of $\Delta Q = 0.1$ and some physical aspects could prompt a deviation ranging from $\Delta Q = 0.1$ to $\Delta Q = 0.2$ [38]. This is a theoretic study that has the advantage of being able to isolate and analyze the variables desired, i.e. in this case pupil size, optical zone, and initial degree of hyperopia. Of course, the practical effects during corneal ablation could alter the theoretic results presented here. In addition, we have not used a customized eye model [39] that can include real data from patients, but we must take into account that many clinics use Q-optimized algorithms because they do not have experimental devices to measure many of the relevant eye parameters nor specific software to manage a customized corneal ablation.

In summary, the results shown here indicate that in the case of correcting hypermetropia by refractive laser surgery, the value of final asphericity around Q = –0.18 provides good theoretical visual quality after surgery under a broad variety of clinically important experimental conditions: initial level of hyperopia, pupil size and different optical zones.

Funding

This work was supported by Ministry of Economy and Competitiveness (Spain) and European Regional Development Fund (ERDF) (Grant FIS2013-42204-R).

Acknowledgments

We thank David Nesbitt for translating the text into English.